Physica D 70 (1994) 321–341
North-Holland

SSDI: 0167-2789(93)E0290-R

PHYSICA D

Vulnerability in one-dimensional excitable media*

Joseph Starobin, Yuri I. Zilberter and C. Frank Starmer

Departments of Medicine (Cardiology) and Computer Science, Duke University Medical Center, Durham, NC 27710, USA

Received 23 June 1993
Revised manuscript received 20 September 1993
Accepted 23 September 1993
Communicated by A.V. Holden

Potentially life-threatening cardiac arrhythmias can be initiated with stimuli timed to occur during the "vulnerable window (VW)". We defined VW as the time interval between the "conditioning" and "test" stimuli following in sequence, during which the test stimulus response propagates in only one direction. We show that the VW is a generic feature of excitable media and describe the relationship between the properties of an excitable medium and the VW. We present asymptotic results that reveal the sensitivity of the VW to both the propagation velocity of the conditioning wavefront and the recovery process parameters. We also have identified a critical length of medium that must be excited in order to reveal vulnerability. Analytical results are in agreement with numerical studies.

1. Introduction

Normally, cardiac tissue is quiescent and a wavefront is formed only when a special pacemaker cell "fires" and excites adjoining cells. At a critical time following the passage of this wavefront, cardiac tissue can be stimulated again such that a self-maintained, reentrant (spiral) wavefront of excitation is indicated. Often this alteration in cardiac rhythm is life-threatening, leading to ventricular fibrillation and sudden cardiac death [1,2]. The range of critical times is referred to as the "vulnerable period" (VP). Recently Winfree [3] has referred to vulnerability as a sort of "black hole" in the phase-plane representation of the reaction-diffusion equations that characterize an excitable medium such as cardiac tissue. Theoretical [4,5] studies and *in vitro* experiments [6] have shown the excitation wavefront associated with these altered rhythms to be that of a spiral wave – similar to that observed in other excitable media. Although there are many published reports of spiral waves and their evolution (quasi steady-state behavior), there are almost no results about the initiating events and no analytical studies of vulnerability as defined by experimental studies in cardiac tissue.

Recently, a large clinical trial of several antiarrhythmic drugs was terminated because the treated group experienced a 3 fold increase in the rate of sudden cardiac death compared with a control, untreated, group [7], perhaps a reflection of increased cardiac vulnerability. We studied the one-dimensional analog of the VP, the vulnerable window (VW) and suggested that drug alteration of medium excitability (by blockade of cellular membrane sodium channels) can prolong the vulnerable window [8,9].

How are spiral waves initiated in an excitable

* Supported in part by NIH research grants HL32994 from the National Heart, Lung and Blood Institute and TW00345 from the Fogarty International Center.

medium and how is this related to vulnerability? It is well known that one can initiate a spiral wave by disrupting a continuous wavefront [10,11]. A break in the wavefront can be created by a collision between the wavefront and an obstacle in its path [10]. Alternatively, wavefront formation can be partially inhibited at the time of its initiation, i.e. stimulation under certain conditions will produce a discontinuous wavefront. Such incomplete wavefront formation results when excitability in the region of the stimulation site is anisotropic [12]. In a homogeneous medium, for instance, anisotropic excitability exists in the region of a stimulation site, s2, when a conditioning wavefront, initiated by stimulation at a different site (s1), passes over it (fig. 1). This is often referred to as functional anisotropy.

Wiener and Rosenblueth first proposed the concept of functional anisotropy in studies of self-maintained circulation of a pulse around a ring of homogeneous excitable medium [12]. The medium at equilibrium initially exhibited uniform excitability. It was then disturbed by passage of a conditioning wavefront. A test stimulus was applied at a location different from the conditioning stimulation site and at a time when formation and propagation of the test wavefront was permitted in only one direction. The resulting wavefront circulated continuously around the loop.

Later analytical and numerical studies determined that there was a minimum ring length (pulse duration × conduction velocity) that was necessary for maintaining circulation [13,14]. In 2-D, these estimates approximated the dimensions of the core of the spiral as revealed by numerical simulations [15]. Analytical approximations of the 2-D spiral wave behaviour are given in refs. [16,17].

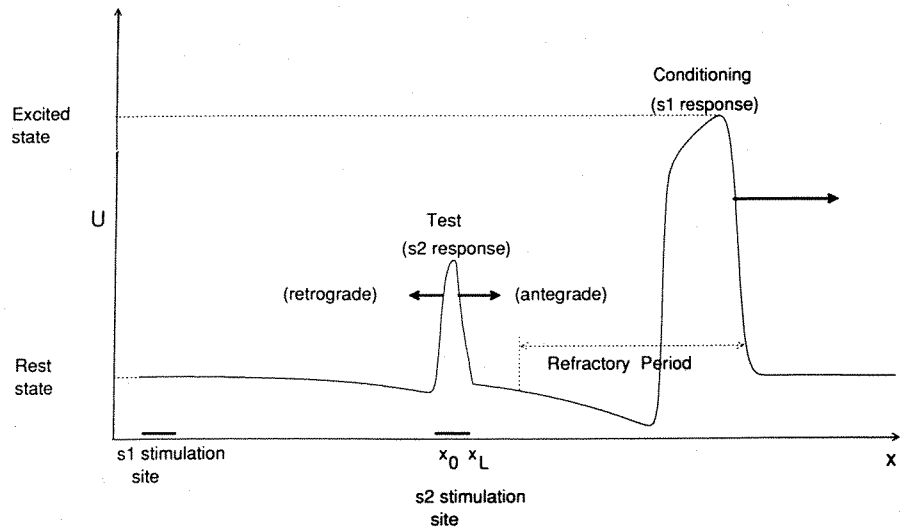

Fig. 1. One-dimensional model for exploring the vulnerable window. Shown is a 1-D cable of Fitzhugh–Nagumo excitable medium. There are two stimulation sites: s1 is activated to initiate a conditioning wavefront that propagates from left to right, and s2 is activated to test the excitability of the medium. For a typical study, the s2 electrode is activated after activation of the s1 site, in order to provide time for the conditioning wavefront to pass off the s2 site. Three classes of responses are possible. For short s2 − s1 delays, the conditioning wavefront will not reach the s2 site so that bidirectional conduction of the test wavefront will be observed. Similarly, for long s2 − s1 delays, the effect of the conditioning wavefront on excitability near the s2 site will be negligible so that bidirectional conduction of the test wavefront will occur. For intermediate s2 − s1 delays when the conditioning wavefront is passing off the s2 site, the medium is inexcitable and propagation of the test wavefront will not be observed. However, for slightly longer s2 − s1 delays, the medium to the right of the s2 site will be inexcitable while the medium to the left of the s2 will be excitable and a unidirectionally propagated test wave will be observed.

In these studies, most investigators probed wavefront propagation after a discontinuity had already been established, often with the use of obstacles. Except for the pioneering work of Wiener and Rosenblueth [12], very little attention has been given to describing the conditions under which unidirectional block of wave propagation (formation of a discontinuous wavefront) can be achieved in a homogeneous medium. The initial analytical observations of Wiener and Rosenblueth [12] in a one-dimensional medium suggest that spiral-like patterns can be initiated in a homogeneous medium. Later studies by Gul'ko and Petrov [4] confirmed these early hypotheses.

We use the term, excitable, to refer to media where the state of a region, subjected to a single suprathreshold perturbation, switches from an "equilibrium" state to an "excited" state and then slowly returns to the equilibrium state. Under most conditions, the excited region forms continuous wavefronts that propagate in all directions in response to the diffusion process. Vulnerability, on the other hand, refers to a spatial distribution of excitability of the medium such that the excitatory wavefront is incompletely formed and propagation fails in some directions.

One typical example of the vulnerability is given in the work of Wiener and Rosenblueth [12]. They studied the problem of initiating a continuously circulating pulse in a one-dimensional ring of an excitable medium, stimulating the medium by two timed stimuli ("conditioning" and 'test") following in sequence. This study showed that vulnerability is revealed only when a wavefront successfully forms and propagates in one direction but fails in another direction and that only under this condition a continuous pulse circulation in an excitable ring is possible. The importance of such a condition for the initiation of a continuous pulse circulation has also been shown in refs. [18,19], where the authors studied the initiation of reentry in two coupled excitable fibers.

In accordance with the above we define vulnerability in terms of the medium state where test stimulation, which follows the conditioning stimulation and is applied to the region with incomplete recovery, results in a response that is propagated in some directions and fails to propagate in other directions. We have limited the distribution of excitability in the medium to that generated by the passage of a conditioning wavefront. This conditioning wavefront is used to explore vulnerability in both cardiac tissue studies [20] and in patients that exhibit heart rhythm disturbances [21,22].

Vulnerability can be readily visualized (fig. 1). A conditioning wavefront is initiated at the s1 site. As the conditioning wavefront passes over the s2 stimulation site, the medium properties change from fully excitable (in a rest state), to absolutely refractory (during the time the pulse travels over the s2 site) to relatively refractory (as the medium recovers its excitability). There is a critical point during the relative refractory period of the conditioning wavefront where the medium in the antegrade direction is unable to support wavefront formation while the medium in the retrograde direction can support wavefront formation and propagation.

In cardiac tissue, wavefront propagation can begin as the result of excitation of a few cells suggesting that a few cell lengths may be comparable to the thickness of a developed wavefront. As mentioned in ref. [23] human atrial and ventricular cells are of the order 6–10 μm and 10–20 μm in diameter, respectively, and are approximately of the same length which is of the order 60–150 μm. Most mammalian cardiac tissue studies show that propagation velocity is $0.5–1\ \mathrm{m\,s^{-1}}$, where the lower bound corresponds to the atrium [24] and the upper bound corresponds to the ventricle [25].

Wavefront formation time is approximately the same as the time constant of an inward excitation sodium current which is of the order of 0.3 ms [26]. For example, if 0.3 ms is the approximate time required for wavefront forma-

tion, then the approximate atrial and ventricular wavefront thickness is of the order of 150 μm and 300 μm, respectively, the length less than 3 cells for atrium and less than 5 cells for ventricle. Consequently, we will adapt our analysis to consider electrode lengths comparable to those of myocardial cells.

To fix ideas, we will use stimulation protocols often used in experiments to drive our analytical considerations, i.e. stimulation protocols where the state of the medium is shifted from a homogeneous state to some time-dependent nonhomogeneous state by the passage of a conditioning wavefront. Our probe for vulnerability will be limited to test stimuli that are delayed to occur at different times following the passage of the conditioning wavefront. The size of the test electrode range in size from a fraction of the wavefront thickness to several wavefront thicknesses.

We will define the vulnerable window (VW) as the range of time delays between a conditioning stimulus and a test stimulus where the test stimulus response is propagated in only one direction (retrograde propagation) (fig. 1). To identify the VW under these conditions, we will explore the formation and propagation of two nonstationary waves which are produced by test stimulation. These two nonstationary waves can either successfully develop and propagate or one or both may fail to develop and propagate, depending on spatial pattern of medium excitability. In this paper the analysis will be based on a one-dimensional approximation of the Fitzhugh–Nagumo model.

2. Model

Our problem is motivated by one-dimensional cable models of an excitable fibre. These models are of the form

$$C_m\,\partial\phi/\partial t = I(\mathrm{Na}) + I(\mathrm{K}) + I(\mathrm{stim}) + D\,\partial^2\phi/\partial x^2\,,$$

where ϕ is the cellular membrane potential, C_m is the membrane capacitance, $I(x)$ are ionic and stimulation membrane currents and D is the diffusion coefficient. Each individual membrane current $I(x)$, is expressed as the product of a conductance and a driving force, $\sigma_x(\phi - \phi_x)$. Krinsky and coworkers [27] reduced the Hodgkin–Huxley equations to a variable description for an excitable fibre (Fitzhugh–Nagumo-like description) which is similar to the one mentioned above.

Antiarrhythmic drugs and antiseizure drugs alter cellular excitability and have been shown to reduce ionic conductances, σ_x [28–30]. Moreover, these drugs have been shown to simultaneously suppress spiral formation under some conditions and amplify the likelihood of spiral formation under other conditions [8,9,31]. For this reason, it is interesting to explore the determinants of the vulnerable window so that the action of these drugs might be better understood.

A two variable Fitzhugh–Nagumo-like representation of an excitable fibre with an inward excitation current ($I_{\mathrm{Na}} = \sigma_{\mathrm{Na}} f(u)$) and a slower outward recovery current ($I_{\mathrm{K}} = V$) is given by

$$C_m \frac{\partial u}{\partial t} = V - \sigma_{\mathrm{Na}} f(u) + D \frac{\partial^2 u}{\partial x^2}\,,$$

$$\frac{\partial V}{\partial t} = \frac{-(\sigma_{\mathrm{K}} u + V)}{\tau_{\mathrm{K}}}\,,$$

where σ_{Na}, σ_{K} are the maximum sodium and potassium conductances, respectively, and τ_{K} is a time constant of a slow recovery process.

Let us consider this system in dimensionless form:

$$\frac{\partial u}{\partial t} = \frac{\partial^2 u}{\partial x^2} + V - f(u)\,, \tag{1}$$

$$\frac{\partial V}{\partial t} = \varepsilon(-\gamma u - V)\,. \tag{2}$$

Here $u(x,t)$ is a dimensionless membrane potential, $V(x,t)$ is a dimensionless slow recovery

current. The scale of u is the maximum action potential amplitude U_0, the scale of V is given by $\sigma_{Na}U_0$ and the scale of time is C_m/σ_{Na}. The character length scale L is given by $(D/\sigma_{Na})^{1/2}$ and, as mentioned above, is of the order of 150–300 μm. The small parameter, $\varepsilon \ll 1$, is equal to $C_m/(\tau_K\sigma_{Na})$ and $\gamma = \sigma_K/\sigma_{Na}$.

The system (1), (2) represents a standard excitable reaction-diffusion process where the function, $f(u)$, exhibits a negative resistance region. The nature of the solution is determined by the intersection of the two nullclines (fig. 2). Two important values of the recovery variable will be used in our analyses: V_{eq} is the equilibrium value of the slow variable and is determined by the intersection of the nullclines; V_{crit} is the critical value of the recovery that separates propagated responses from nonpropagated responses. The parameters, m_1, m_2 and m_3, are the roots of $f(u)$ relative to $V = V_{eq}$. The responses of both the fast variable, u, and the slow variable, V, to stimulation are shown in fig. 3 for a stable equilibrium at m_1. Here we show both the fast (u) and slow (V) variables in response to both a conditioning stimulus and a test stimulus.

When the medium is at the equilibrium, $(u(x, t=0) = m_1)$, and $u(\mathrm{s1}, t_{cond})$ is transiently changed by a sufficient amount (stimulation), then a conditioning action potential is initiated that propagates away from the point of stimulation (s1). On a much slower time scale, V slowly becomes more negative with respect to V_{eq} and inhibits the formation of the u wavefront. Test stimulation at a point, s2, while $V(\mathrm{s2}, t_{test}) < V_{crit}$ will not produce a response, and the medium is said to be refractory. However, delaying test stimulation such that $V(\mathrm{s2}, t_{test}) > V_{crit}$, stimulation can again produce a propagated response.

The success or failure of propagation at $x = \mathrm{s2}$ depends on the value of $V(\mathrm{s2}, t_{test})$. We can readily visualize the vulnerable window by observing the nature of a propagated wavefront initiated as the point, S, moves from left to right where S is the point where $V(x, t) = V_{crit}$. When S is to the left of s2, propagation fails in both directions. When S is to the right of s2, propagation succeeds in both directions. However while S travels across the s2 electrode, a wavefront can propagate to the left but fails to propagate to the right. If the electrode length is sufficiently large that one can neglect the effects of wavefront formation, the duration of the vulnerable window can be approximated by L_S/C where L_S is the electrode length and C is the propagation velocity of the conditioning wavefront [32].

3. Methods

We solved the system (1), (2) numerically by using the implicit difference scheme with second-order approximation on the space grid interval, Δx, and first-order approximation on the time grid interval, Δt. The accuracy of the numerical results, $u_{i\,\Delta x}$, was assessed as $\max(i)\|u_{i\,\Delta x} - u(x)\| = \eta\,\Delta x^2$ where $u(x)$ is the exact solution. With numerical experiments, we computed a grid solution for space steps of Δx, $\Delta x/2$ and $\Delta x/4$. We measured the maximum difference of $u_{i\,\Delta x}$ for corresponding points on each grid. The slope, η, of the $\max(u_{i\,\Delta x})$ as a function of Δx^2 was 2.14.

To compare numerical and analytical results relating to wavefront properties, it is necessary to define the endpoints of a wavefront. Since the precision of our numerical studies was bounded by $\eta\,\Delta x^2$, we used this quantity as a threshold for defining the beginning and the end of a wavefront. We defined the beginning of the wavefront to occur when $u(x, t)$ crossed the threshold, $m_1 + \eta\,\Delta x^2$, and the end of the wavefront to occur when $u(x, t)$ crossed the threshold, $m_3 - \eta\,\Delta x^2$. The values of grid intervals used for all numerical experiments, Δx and Δt, were 0.1 and 0.01, respectively.

Vulnerability can readily be demonstrated with numerical experiments by varying the s2 − s1

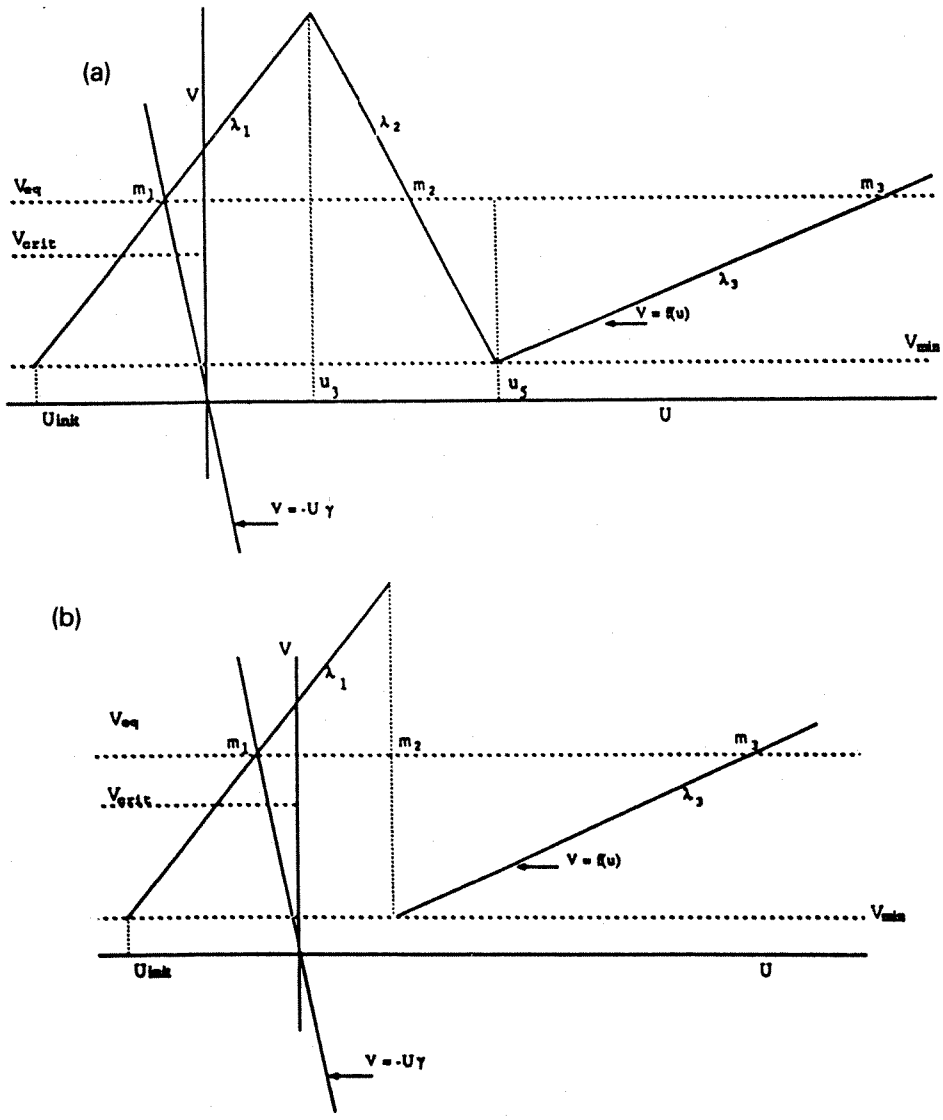

Fig. 2. Null-clines of an excitable medium described by eqs. (1) and (2). Panel (a) illustrates a piecewise approximation $f(u)$ with different slopes λ_1, the negative resistance region, λ_2, and λ_3. In panel (b) is shown the idealized $f(u)$ with different λ_1 and λ_3 and where $\lambda_2 = \infty$ for analytical convenience. Unless otherwise noted, our numerical results were obtained with $\lambda_1 = \lambda_3 = 2.0$, $\gamma = 8.0$. With these values, $V_{eq} = 6.4$, $V_{crit} = 4.9$, $m_1 = -0.8$, $m_2 = 0.05$, $m_3 = 2.4$, $\varepsilon = 0.006$.

stimulus delay and observing the response to test stimulation (fig. 4). The transition between decay of the test wavefront in both antegrade and retrograde directions and unidirectional conduction is shown in figs. 4a,b. In these experiments, $x_{ts} = s2 - s1$ delay was varied by moving the site of the s2 stimulation. Note that a very small change in the s2 site resulted in a sharp transition between decaying conduction (a) and unidirectional conduction (b). Similarly in panels (c) and (d), one can see the transition between unidirectional propagation of the test wavefront and stable, bidirectional conduction.

We will explore vulnerability analytically by characterizing the formation of a wavefront under stationary (for the conditioning wave-

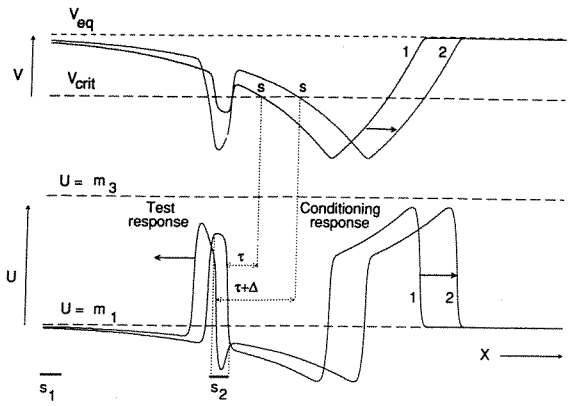

Fig. 3. Detailed representation of a 1-D excitable cable that illustrates the responses to conditioning and test stimulation. First, the medium is stimulated at the left electrode, s1. The resulting u wavefront, 1, is propagated to the right. The recovery "front", V, propagates to the same direction. There is a critical value of the recovery variable, V_{crit}, that determines when the test stimulation results in either successful or failed wavefront formation. As this critical point, S, passes over the test electrode, s2, stimulation will result in a wavefront propagated to the left but not to the right, e.g. a unidirectionally propagated wavefront. The progression of the test wavefront is illustrated shortly after stimulation ($t = \tau$) and then at an later time, $\tau + \Delta$, that shows the asymmetric formation of the front and its propagation.

front) and nonstationary conditions (for the test wavefront). From these results we will estimate the boundaries of the vulnerable window that mark transitions between bidirectional propagation and unidirectional propagation and between unidirectional propagation and no propagation and explore the relationship between the VW and electrode length. Finally, we will estimate the minimum electrode length necessary to reveal vulnerability and compare these results with numerical studies.

4. Calculation of the wave propagation velocity and the structure of the fronts

The system (1), (2) can be solved by the singular perturbation method. Using this method we divide the problem into two sub-problems: the first is the fast process (eqs. (3) and (4)) that describes the formation and propagation of the excitation wavefront; the second (eqs. (5) and (6)) describes the slow recovery process at locations remote from the wavefront (for detail see review [33]):

$$\frac{\partial u}{\partial t} = \frac{\partial^2 u}{\partial x^2} + V - f(u)\,, \tag{3}$$

$$V = \text{constant}\,, \tag{4}$$

$$V = f(u)\,, \quad t = t'/\varepsilon\,, \tag{5}$$

$$\frac{\partial f(u)}{\partial t'} = -\gamma u - f(u)\,. \tag{6}$$

In order to determine the nature of $u(x, t)$ for a solitary pulse, we will first identify the velocity of a solitary pulse. In a zero-order approximation of ε (singular limit), the propagation velocity, Θ, of a solitary pulse coincides with the velocity of a trigger wave (the "ignition" wave without the recovery process [34]), C, which is a function of the constant value of the slow variable, V, as described by eqs. (3) and (4). Adding the first-order term reduces the velocity, a result of introducing time dependent changes in the recovery variable, V, so that [34]:

$$\Theta = C(1 - \zeta_0 \varepsilon)\,. \tag{7}$$

In the singular limit when $\varepsilon = 0$, Θ and C are equal.

Following the strategy outlined in [35, 36] we will find independent zero-order solutions for eqs. (3) and (4) (that describe wavefront formation with a fast time scale) and eqs. (5) and (6) which describe the much slower recovery process. To obtain an analytical solution of (3)–(6) we will utilize a piecewise approximation of $f(u)$ and will find the velocity C solving (3) and (4), (5), (6) separately (fig. 2a).

Changing the variables in (3): $\xi = x - Ct$, $\varphi = \mathrm{d}u/\mathrm{d}\xi$, we get

$$\varphi\left(\frac{\mathrm{d}\varphi}{\mathrm{d}u} + C\right) + V - f(u) = 0\,. \tag{8}$$

In order to find the velocity, C, of the trigger wave and its dependence on the value of the

recovery variable, V, it is necessary to find the solution to (8) as a separatrix connecting the two stable equilibrium points $(m_3, 0)$ and $(m_1, 0)$ determined by the roots of $f(u)$ relative to $V = V_{eq}$. It follows from fig. 2 that the solution, φ, can be approximated by two overlapping partial solutions described by

$$\varphi = b_1(u - m_1) \quad \text{if } m_1 < u < u_3 ,$$
$$\varphi = b_3(m_3 - u) \quad \text{if } u_5 < u < m_3 . \tag{9}$$

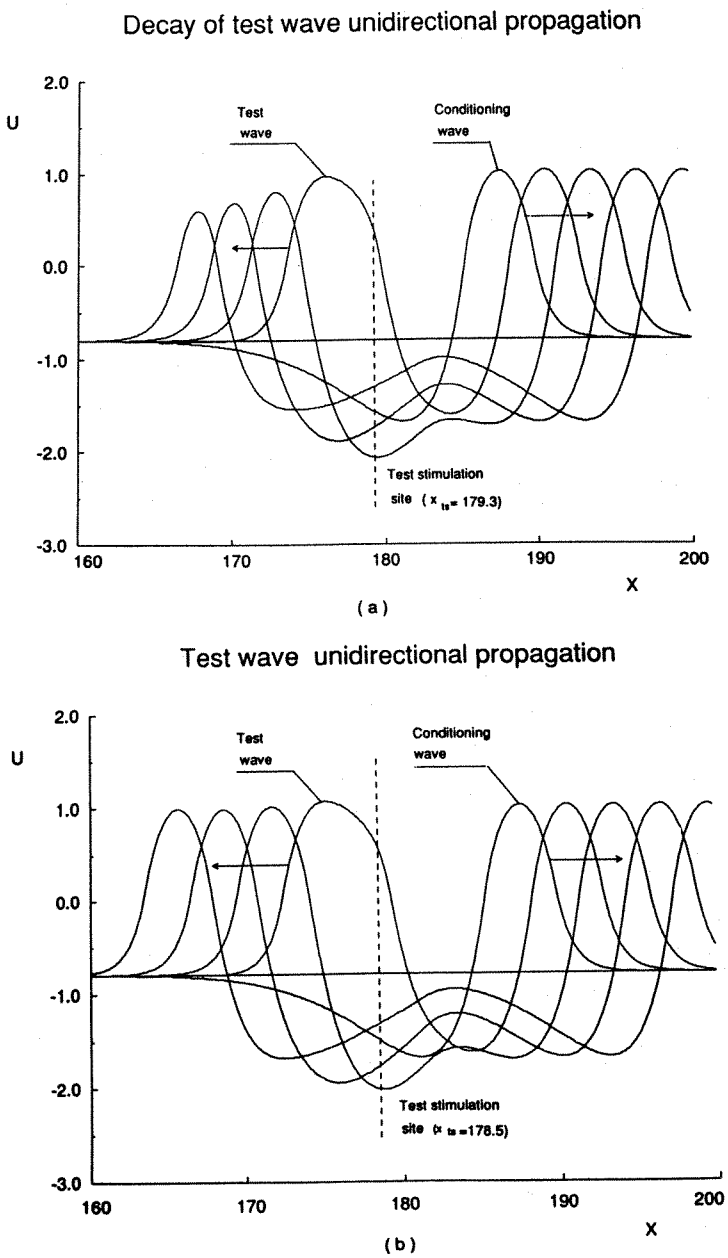

Fig. 4. Numerically computed wavefronts near the boundaries of the vulnerable window ($\lambda_1 = \lambda_3 = 0.5$, $\gamma = 8$, $\varepsilon = 0.006$). Panels (a), (b) illustrate the transition between failed (a) conduction and unidirectional (b) propagation: (a) $x_{ts} = s2 - s1 = 179.3$; (b) $x_{ts} = s2 - s1 = 178.5$. Panels (c), (d) illustrate the transition between unidirectional (c) propagation and bidirectional (d) propagation: (c) $x_{ts} = s2 - s1 = 168$; (d) $x_{ts} = s2 - s1 = 164.5$.

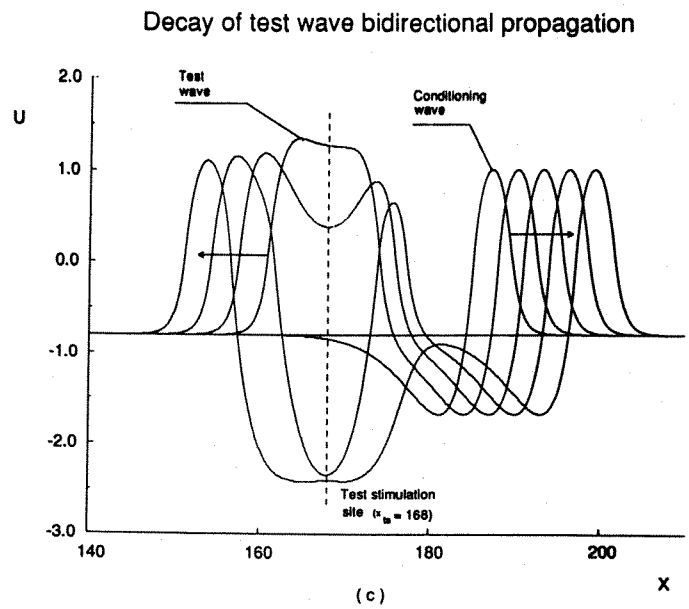

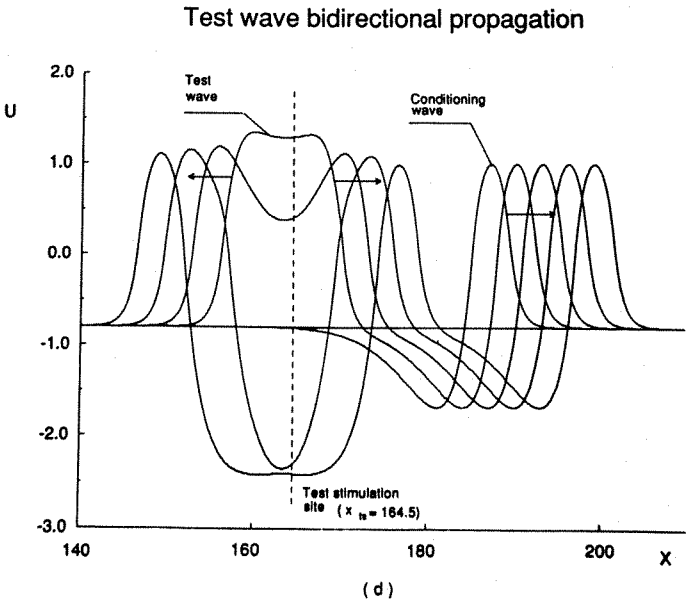

Fig. 4. (Cont'd).

The substitution of (9) in (8) yields

$$b_1 = -0.5C + (0.25C^2 + \lambda_1)^{1/2},$$
$$b_3 = 0.5C + (0.25C^2 + \lambda_3)^{1/2}. \quad (10)$$

In the interval between u_3 and u_5, there exists a solution in the form [37]

$$\varphi = (u - m_2)\psi,$$

where ψ is given by

$$\psi + (u - m_2)\frac{d\psi}{du} = -C - \lambda_2/\psi, \quad (11)$$

with boundary conditions

$$\psi(u_3) = b_1(u_3 - m_1)/(u_3 - m_2)\,,$$
$$\psi(u_5) = b_3(m_3 - u_5)/(u_5 - m_2)\,. \qquad (12)$$

The solution of (11) with boundary conditions (12) yields an expression for the trigger wave velocity, C,

$$\frac{u_3 - m_2}{u_5 - m_2} = \left(\frac{\bar{b}_1 - p_1}{\bar{b}_3 - p_1}\right)^A \left(\frac{\bar{b}_1 - p_2}{\bar{b}_3 - p_2}\right)^B , \qquad (13)$$

where

$$A = \frac{p_1}{p_1 - p_2}\,, \quad B = -A\,, \quad \bar{b}_1 = -b_1\frac{\lambda_2}{\lambda_1}\,,$$
$$\bar{b}_3 = b_3\frac{\lambda_2}{\lambda_3}\,, \quad p_1 = -0.5C + (0.25C^2 - \lambda_2)^{1/2}\,,$$
$$p_2 = -0.5C - (0.25C^2 - \lambda_2)^{1/2}\,.$$

In general it is difficult to solve (13) analytically except for certain simple functional forms of $f(u)$. As in ref. [38] we will consider the case when λ_2 is equal to infinity, but in contrast to [38], we will obtain a solution when λ_1 is not necessary equal to λ_3 (fig. 2b).

When λ_2 is infinite, the solution of (13) yields a wavefront velocity, C, described by

$$C = \pm(\lambda_1 - \lambda_3\alpha^2)/(\alpha(1+\alpha)(\lambda_1 + \lambda_3\alpha))^{1/2}\,,$$
$$\alpha = (m_3 - m_2)/(m_2 - m_1)\,. \qquad (14)$$

Note that when $\alpha = (\lambda_1/\lambda_3)^{1/2}$, the wave propagation velocity, C, is equal to zero. The critical value of the slow variable, $V < V_{\mathrm{crit}}$, is defined by conditions where $C = 0$ and is given by

$$V_{\mathrm{crit}} = V_{\mathrm{eq}} - \lambda_3(m_2 - m_1)\frac{\alpha - (\lambda_1/\lambda_3)^{1/2}}{1 + (\lambda_3/\lambda_1)^{1/2}}\,. \qquad (15)$$

It should be noted that the sign of this inequality must be changed to its opposite if the sign of $f(u)$ is also changed [39].

For later considerations, we will need the dependence of the slow variable on slow time t'. The solution of the slow system (eqs. (5) and (6)) is given by

$$t' = \int_{u_{\mathrm{init}}}^{u} \frac{\mathrm{d}f(u)}{-\gamma u - f(u)}\,. \qquad (16)$$

Since we wish to explore the responses to test pulse stimulation timed to occur in the wake of the conditioning wavefront, it is necessary to describe the behaviour of the slow variable, V, after the back front of the conditioning wave has been formed. The integration of (16) for a piecewise linear function, $f(u)$, when $u_{\mathrm{init}} = m_1 - \lambda_3/\lambda_1\,(m_3 - m_2)$ and $V(u_{\mathrm{init}}) = V_{\mathrm{min}}$ (fig. 2) yields

$$V = -\gamma m_1 - \lambda_3(m_3 - m_2)\exp\left(-\frac{\gamma + \lambda_1}{\lambda_1}t'\right). \qquad (17)$$

Using (15) and (17) one can determine the time, t_{crit}, during which V increases from V_{min} to V_{crit}:

$$t_{\mathrm{crit}} = \frac{\lambda_1}{\lambda_1 + \gamma}\ln\frac{\alpha(1 + (\lambda_3/\lambda_1)^{1/2})}{\alpha - (\lambda_1/\lambda_3)^{1/2}}\,. \qquad (18)$$

To determine the structure of the wave propagation fronts, we solve eq. (9) with boundary conditions given by the expressions $u(-\infty) = m_1$ and $u(\infty) = m_3$. The solution of this boundary value problem is given by

$$u(\xi) = m_1 + K\exp(b_1\xi)\,, \quad u < m_2\,,$$
$$u(\xi) = m_3 - K\exp(-b_3\xi)\,, \quad u > m_2\,. \qquad (19)$$

In order to find K in eq. (19), we must match both $u(\xi)$ and $\mathrm{d}u/\mathrm{d}\xi$ at some intermediate point ξ_*. This matching procedure yields

$$\xi_* = \frac{1}{b_1 + b_3}\ln\frac{b_3}{b_1}\,, \quad K = \frac{m_3 - m_1}{G}\,,$$
$$G = \left(\frac{b_3}{b_1}\right)^{b_1/(b_1+b_3)} + \left(\frac{b_3}{b_1}\right)^{-b_3/(b_1+b_3)}\,. \qquad (20)$$

In accordance with refs. [40, 41] the effective front width, L_0, can be written as $L_0 = (b_1 + b_3)/(b_1 b_3)$. However, the value of L_0 depends on how we define the endpoints of the wavefront, i.e. what is the threshold of u, relative to m_1 and m_3, that defines the boundaries of the wavefront,

$u(x)$. As mentioned above, this threshold can be defined in terms of a small constant, $M = \eta \Delta x^2$, such that the wavefront "starts" when u crosses $m_1 + M$ and "ends" when u crosses $m_3 - M$. Thus the effective front width, L_0, relative to the threshold constant, M, is given by

$$L_0 = \ln(M^{-1}K)\frac{b_1 + b_3}{b_1 b_3}. \tag{21}$$

5. Nonstationary front formation process and calculation of the boundary layer adjustment

Let us consider the process of forming the front of a nonstationary solitary test pulse. The formation of such a wavefront is dependent on the nature of the stimulation amplitude, its duration and the extent of the stimulation electrode. Without limiting the generality of our results, we will consider test stimulation with an amplitude equal to the amplitude of a trigger wave $(m_3 - m_1)$ and specified as an initial condition. For numerical studies, the duration of the stimulus is that of a single time step, Δt. We will consider electrode lengths, L_S, which are greater than the minimum length, L_D, required for formation of a unidirectional response. The evaluation of L_D is given below.

When one considers the zero order approximation (singular limit), the velocities of a trigger wave and solitary pulse are equal to each other, so that the slow and fast solutions for the leading front of the pulse are matched at $u = m_3$ ($V = V_{eq}$).

With a first order approximation, the situation is quite different. It follows from (7) that in a first-order approximation of ε, the propagation velocity of a solitary pulse, Θ, is smaller than the trigger wave velocity C because the recovery process acts to retard development of the wavefront. Since $\Theta < C$ and both the solitary pulse and trigger wave velocities are functions of the slow variable, V, it follows that eq. (7) can be written as $\Theta(V_*) = C(V_{eq})(1 - \xi_0 \varepsilon)$, where $V_* < V_{eq}$ and $C(V_{eq})$ is the trigger wave velocity associated with the equilibrium value of the slow variable, V.

Thus, while the solitary pulse front is forming, the slow variable decreases by some value, δ_V, so that $V_* = V_{eq} - \delta_V$. The reduction of the slow variable in turn leads to a reduction (δ_u) of the front amplitude which, in contrast to a trigger wave, no longer coincides with $(m_3 - m_1)$. In terms of singular perturbation theory, this means that the slow (outer) and fast (inner) solutions must be matched at $u_* = m_3 - \delta_u$ and $V_* = V_{eq} - \delta_V$, where δ_u, δ_V are small corrections (of order, ε) and physically correspond to boundary layer adjustments.

In order to match the fast and slow solutions, we will use a procedure similar to that used for analysis of boundary layers in fluid mechanics [42]. After wavefront formation (during τ) and the front departs from the stimulation site, there is an interval of time during which u follows the nullcline such that $V = f(u)$. From eq. (3), we see that the derivative terms are approximately equal when $V - f(u) = 0$ so that $\partial u/\partial t = \partial^2 u/\partial x^2$. At the point of transition between the completion of the front and initiation of the recovery process, we will replace these derivatives with finite differences relative to the front formation time in terms of the slow time scale, $\tau' = \varepsilon\tau$, and the spatial extent of the front, $x_f - x_b$. Equating these average values of the derivatives in (3), we get the following condition:

$$\Delta u_t/(\varepsilon\tau) = (\Delta u_x(x_f) - \Delta u_x(x_b))/L^2, \tag{22}$$

where Δu_t and Δu_x are the finite time and space increments of u respectively, x_f and x_b are the front and back coordinates of the leading front structure respectively; $x_f - x_b = L$ is the dimensionless diffusion length. The left side of eq. (22) is equal to $-\delta_u$. The first term in the right part is equal to zero since $\partial u/\partial x$ at $x = x_f$ is negligible. The second term $\Delta u_x(x_b)$ is equal to $(m_3 - m_1)$. Noting that the dimensionless diffusion length is equal to one, we get the following expression for

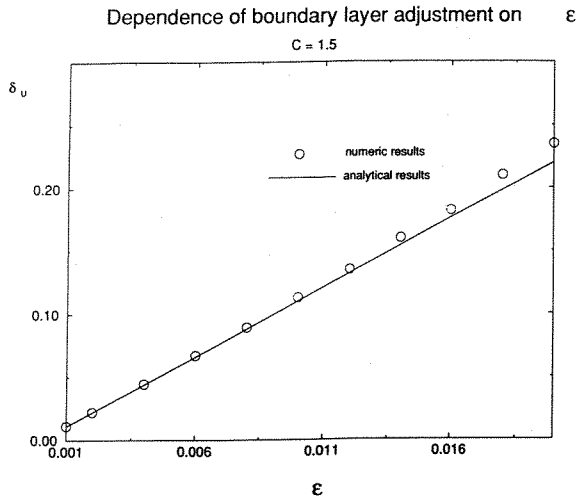

Fig. 5. The dependence of the boundary layer adjustment, δ_u, is linearly related to the relaxation parameter, ε.

correspondence between the boundary layer adjustment, δ_u, and the front formation time, τ:

$$\delta_u = \varepsilon(m_3 - m_1)\tau \,. \tag{23}$$

If $C = \mathcal{O}(1)$ and ε is sufficiently small, then the value of τ can be estimated by L_0/C where L_0 and C are given by eqs. (21) and (14), respectively.

In order to check the approximation used to develop eq. (23), we numerically explored the relationship between ε and δ_u (fig. 5). For $\varepsilon < 0.02$, the analytical evaluation of δ_u was found to be in good agreement with the numerical solution of eqs. (1) and (2).

6. Estimating the vulnerable window

First we will estimate the VW when the size of a test electrode, L_S, is much greater than the wavefront thickness, L_0 (eq. (21)). The behaviour of the VW under these conditions can be described in terms of the singular limit (zero-order approximation), since the wavefront thickness, L_0, is negligible. As mentioned above we define the zero-order approximation of the VW, $\mathrm{VW}^{(0)}$, as equal to time required for the critical point, V_{crit}, of the conditioning wave to pass across the test electrode: $\mathrm{VW}^{(0)} = L_S/C$ [32]. Note that with this approximation, $\mathrm{VW}^{(0)}$ is dependent on all medium parameters, λ and γ, since they both influence the trigger wave velocity, C.

But, as mentioned above, we should also consider the case when the size of the test electrode is of the same order as the thickness of the wavefront given by (21). Under these conditions, the dynamics of wavefront formation may modulate the VW. Let us consider the nonstationary test wavefront formation when $V(\mathrm{s2}, t_{\mathrm{test}})$ is near V_{crit}, a condition that occurs when the medium has not returned to its equilibrium state after passage of a conditioning wave. Here, the formation of the test wavefront is paralleled by the recovery process associated with the conditioning wave as it moves away from test stimulation site. If the size of the test electrode is comparable to the thickness of the wavefront, it is necessary to analyze both of these processes simultaneously, since both the fast and slow processes influence the $V(x)$ gradient in the vicinity of V_{crit}. Furthermore, if the test wavefront formation time, τ, is sufficiently small, then these two processes can be represented by a linear approximation. From a physical perspective in this approximation, during front formation we have competition between two linear (in time) processes: an "amplifying" recovery process (the residual recovery from passage of the conditioning wavefront) which yields an increase (greater excitability) of the slow variable by ΔV_+ and an "attenuating" process associated with wavefront formation of the test wavefront, during which the slow variable decreases (less excitability) by a value ΔV_- equal to the boundary layer adjustment $\delta_V (\Delta V_- = \delta_V)$.

If the resulting value of the attenuating process, δ_V, associated with front formation is greater than the increase of the slow variable due to recovery, ΔV_+, then a unidirectionally propagated wavefront (incomplete formation of the test wavefront) occurs in response to test stimu-

lation. A unidirectional response occurs because as the test wavefront forms, the inequality $\Delta V_- > \Delta V_+$ remains valid, such that the slow variable on at least one side of the test stimulation site is less than V_{crit} and the wavefront developing on this side of the test stimulus fails to propagate. The result from the recovery process, ΔV_+ can be approximated by the linear term in Taylor's expansion of V (eq. (17)) in the vicinity of t_{crit} (eq. (18)):

$$\Delta V_+ = \xi_1 \Delta t' ,$$

$$\xi_1 = \frac{\lambda_3}{\lambda_1}(m_3 - m_2)(\gamma + \lambda_1) \times \frac{\alpha - (\lambda_1/\lambda_3)^{1/2}}{\alpha(1 + (\lambda_3/\lambda_1)^{1/2})} . \quad (24)$$

Here $\Delta t'$ is an increment of the slow time in the vicinity of t_{crit}. The resulting value of the attenuating process, δ_V, can also be found by linear approximation. In this approximation the derivative, $\partial V/\partial t(t_{crit})$, is equal to a constant for time in the vicinity of t_{crit}. Equation (6) in this case yields the relationship between δ_u and $\delta_V : \delta_V = \gamma\delta_u$, where δ_u is given by eq. (23).

Let us consider the balance of the attenuating and amplifying processes in detail (fig. 6). As mentioned above, we have placed the test stimulation in the region where the medium is not fully recovered. In other words, the test stimulus is imposed in a region with a gradient of the slow variable. After stimulation, part of the test impulse will form in the region to the left of point S, where $V(x < S, t > t_{test}) > V_{crit}$, while the other part will form to the right of S, where $V(x > S, t > t_{test}) < V_{crit}$ (figs. 6a,b). Depending on time delay, T, between the moment of test stimulation, t_{test}, relative to the moment t_m of passage of the critical point, S, over the midpoint of the electrode, one can produce no response, unidirectional conduction of the test wave (delay = T_1) or bidirectional conduction (delay = T_2). The time, t_{test}, in both cases is equal to $t_m - T_1$ and $t_m + T_2$, respectively.

When $L_S < 2L_{crit}$, we hypothesize that both delays, T_1 and T_2, are less than L_{crit}/C (fig. 6), where L_{crit} can be determined from (20), (21) and (10) where C is given by (14):

$$L_{crit} = \ln[M^{-1}K_1]\frac{\lambda_1^{1/2} + \lambda_3^{1/2}}{(\lambda_1\lambda_3)^{1/2}} ,$$

$$K_1 = \frac{m_3 - m_1}{G}\left[1 - \frac{(\alpha - (\lambda_1/\lambda_3)^{1/2})(\lambda_1 - \lambda_3)}{\lambda_1(1+\alpha)(1 + (\lambda_3/\lambda_1)^{1/2})}\right] . \quad (25)$$

We will also hypothesize that the mutual interaction of the test and conditioning waves is significant only while the critical point, S, of the conditioning wave moves a distance less than the thickness of a fully developed test impulse, $2L_{crit}$, after the moment of the test stimulation (fig. 6). Therefore, a slow time increment $\Delta t'$ in (24) is equal to $\varepsilon(2L_{crit}/C)$. With these considerations, we can formulate the conditions for determination of boundaries of the vulnerable window as defined by the delays, T_1 and T_2.

For the boundary between failed propagation and unidirectional conduction consider the events shown in fig. 6a. The boundary separating failed propagation from unidirectional propagation occurs for the time of test stimulation, $t_m - T_1$, where $V(P, t_m - T_1) > V_{crit}$ at the left boundary of a potentially fully developed test impulse (e.g. where $u(x, t)$ crosses the threshold, $m_1 + M$) decreases to the critical level, V_{crit}, during a fast time $2L_{crit}/C$ which is necessary for point S to move a distance $2L_{crit}$ from the initial location at the moment of the test stimulation. In terms of a fast time, the equation of the balance of amplifying and attenuating processes is the following: PU + PQ − PD = 0 (fig. 6a). Here PU = ΔV_+, PD = ΔV_- and PQ are given by:

$$\Delta V_+ = \left(\frac{2L_{crit}}{C} - \frac{L_s}{C}\right)\xi_1 ,$$

$$PQ = \left(\frac{L_{crit}}{C} - T_1 - \frac{L_s}{2C}\right)\xi_1 ,$$

$$\Delta V_- = \gamma(m_3 - m_1)\left(\frac{L_{crit}}{C} + T_1 - \frac{L_s}{C}\right) . \quad (26)$$

Factor ξ_1 is given by (24). Here the duration

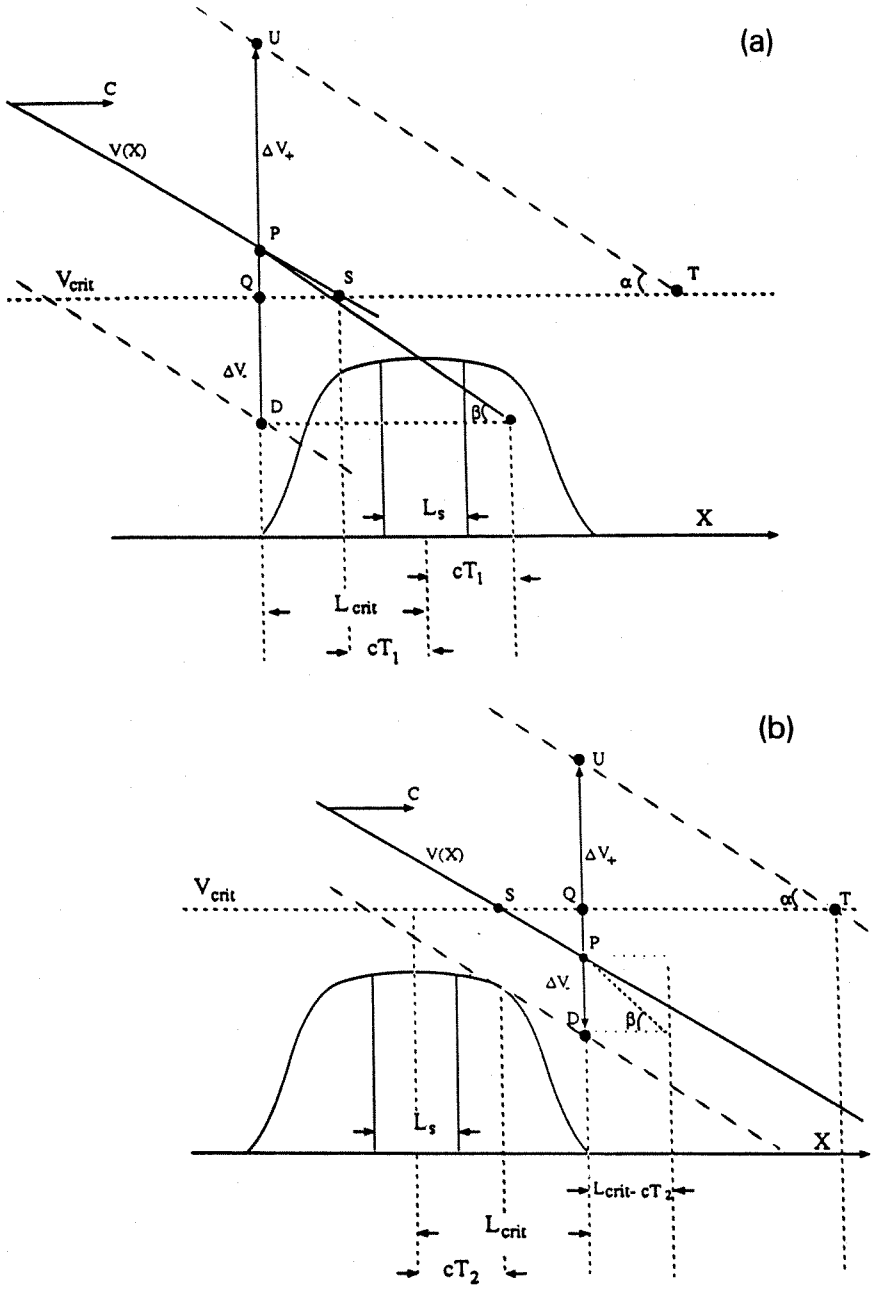

Fig. 6. Role of the propagating front, $V(x)$, when the point, S, representing the critical recovery value necessary for successful wavefront formation, V_{crit}, passes across the region of the electrode. Shown is the test electrode (length = L_s) and the fronts that are being formed at the left and right boundaries. The recovery parameter is shown as a linear approximation. The development of the front during the propagation of S is dependent on the balance of the attenuating, ΔV_-, and the amplifying, ΔV_+, effects.

of attenuating process is determined by the fraction of $2L_{crit}/C$ $(L_{crit}/C + T_1)$ when the point, S, crosses the region of test impulse formation. The time during which the conditioning wave travels a distance equal to the length of the electrode has not been taken into considera-

tion in the balance equation, because we considered the stimulation field as constant in the vicinity of the electrode.

Transforming the above equations, we get the expression for T_1:

$$T_1 = \frac{1}{1+\xi}\left[\left(\frac{3L_{crit}}{C} - \frac{3L_S}{2C}\right)\xi - \frac{L_{crit}}{C} + \frac{L_S}{C}\right],$$

$$\xi = \frac{(\gamma+\lambda_1)}{\gamma(1+\alpha)}\frac{\lambda_3}{\lambda_1}\frac{\alpha - (\lambda_1/\lambda_3)^{1/2}}{1+(\lambda_3/\lambda_1)^{1/2}}. \quad (27)$$

For the boundary between unidirectional and bidirectional conduction, consider the events shown in fig. 6b. The boundary separating unidirectional propagation from the bidirectional one occurs at the time of the test stimulation, $t_m + T_2$, where $V(P, t_m + T_2) < V_{crit}$ at the right boundary of a potentially fully developed test impulse increases to the critical level, V_{crit}, during the time $2L_{crit}/C$. The balance of amplifying and attenuating processes is the following: PU − PQ − PD = 0 (fig. 6b). The value ΔV_+ is the same as above. The expressions of ΔV_- and PQ are given by:

$$PQ = \left(\frac{L_{crit}}{C} - T_2 - \frac{L_s}{2C}\right)\xi_1,$$

$$\Delta V_- = \gamma(m_3 - m_1)\left(\frac{L_{crit}}{C} - T_2 - \frac{L_s}{C}\right).$$

Here the duration of the attenuating process is determined by the fraction of $2L_{crit}/C$ ($L_{crit}/C - T_2$) when the point, S, crosses the region of the test impulse formation. Transforming these equations, we get the expression for T_2:

$$T_2 = \frac{1}{1+\xi}\left[-\xi\left(\frac{L_{crit}}{C} - \frac{L_s}{2C}\right) + \frac{L_{crit}}{C} - \frac{L_s}{C}\right]. \quad (28)$$

Combining (27) and (28) and adding the time, L_S/C, required for S to cross the length of the electrode, we get the piece-wise expression for the vulnerable window:

$$VW^{(0)} = L_S/C, \quad L_S > 2L_{crit},$$

$$VW = \frac{1}{C}\left(\frac{L_s}{1+\xi} + L_{crit}\frac{2\xi}{1+\xi}\right),$$

$$L_D < L_S < 2L_{crit},$$

$$VW = 0, \quad L_S < L_D. \quad (29)$$

The dependence of the VW on L_S is shown in fig. 7, illustrating the departure for small electrode sizes from linearity as defined by the singular limit slope. The VW is zero for electrode lengths less than a critical length, L_D, which was determined numerically and is equal to $0.22L_{crit}$ in the particular case where $\lambda_1 = \lambda_3 = 2$, $\varepsilon = 0.006$ and $\gamma = 8$ (as mentioned above the amplitude of the stimulus is equal to $m_3 - m_1$). For lengths, $L_D < L_S < 2L_{crit}$, the VW is proportional to the front formation time of the test impulse. For longer electrodes where $L_S > 2L_{crit}$, the VW asymptotically approaches to $VW^{(0)} = L_S/C$. Moreover, eq. (29) illustrates the generic nature of vulnerability and shows the dependence of the VW on all medium parameters.

Numerical experiments (fig. 7) revealed good agreement with the analytical solution (eq. (29)). The numerical estimates of the VW were determined by using a binary search of candidate delays between conditioning and test stimulation. The delay was implemented by moving the test stimulation site.

We also explored the sensitivity of the VW to the medium parameters. For $\lambda_1 = \lambda_3 = 2$, $\varepsilon = 0.006$ the difference between numerical and analytical dependencies of the VW on the slow conductance, γ, was less than 5% if V_{crit} was sufficiently different from V_{eq} (fig. 8). The same behaviour can be seen for the dependence of the VW on the fast conductance (fig. 9). In this case, the slopes, λ_1 and λ_2 are equal to each other. The dependence of VW on γ, λ_1, λ_3 for different slopes is shown in fig. 10 ($\lambda_1 = 2$). As mentioned above there is a significant difference between the numerical and analytical results only when V_{crit} is sufficiently close to V_{eq}: $\beta = (V_{eq} - V_{crit})/V_{eq} < 0.1$ (figs. 8, 9).

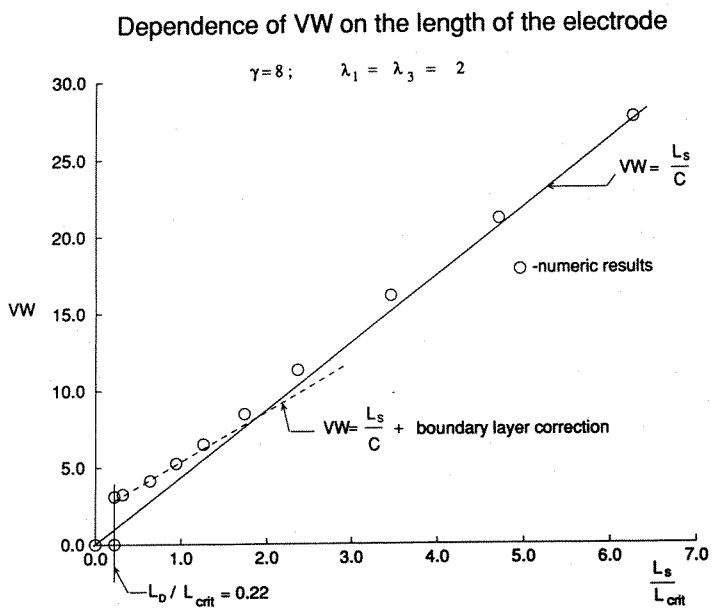

Fig. 7. The dependence of the duration of the vulnerable window on the length of the electrode. Shown in units relative to the front thickness, L_{crit}, are numerically and analytically determined values of the VW for electrode lengths ranging from less than the minimal length necessary for unidirectional propagation (L_D) to lengths comparable to several front lengths ($7L_{crit}$). For lengths greater than $2L_{crit}$, the singular limit approximation is adequate to describe the dependence of the VW on medium parameters. There is a sharp transition at $L_S = L_D$ that reflects the minimal requirements for unidirectional propagation (ignition). For electrode lengths less than $2L_{crit}$, the VW duration is greater than that associated with the singular limit, L_S/C, and is described by the boundary layer correction.

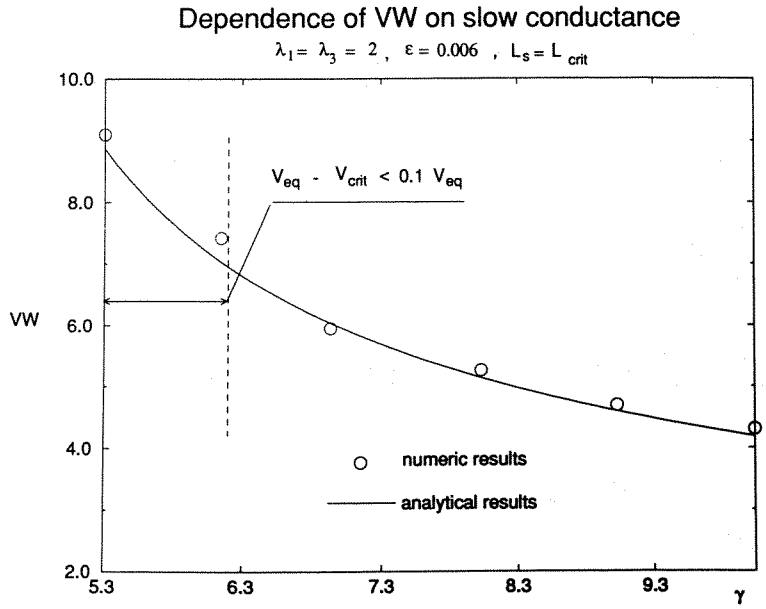

Fig. 8. Dependence of vulnerable window on slow conductance γ.

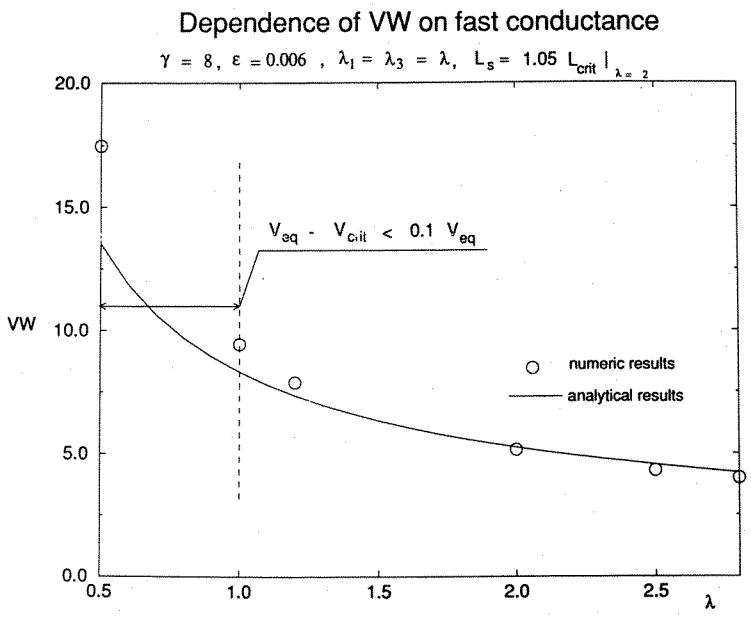

Fig. 9. Dependence of vulnerable window on fast conductance λ ($\lambda = \lambda_1 = \lambda_3$).

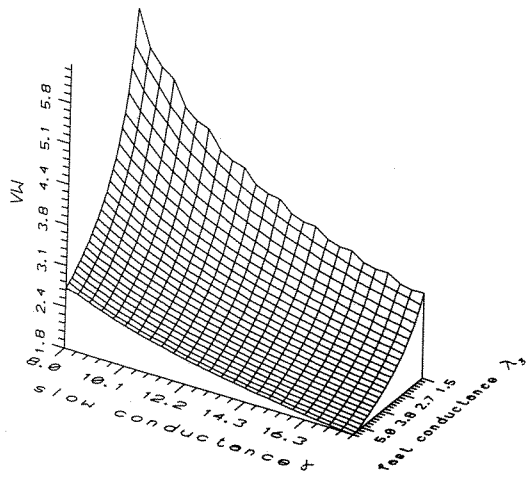

Fig. 10. Dependence of vulnerable window on slow conductance γ and fast conductance λ_3 for $\lambda_1 = 2$.

The derivation of eq. (29), based on a linear superposition of recovery and test wavefront formation processes, appears valid over a wide range of β. If $\beta < 0.1$, the test wavefront formation time, τ, is large enough so that it is no longer comparable to the fast time scale. This means that in this range of β, the separation of the system (1), (2) into slow and fast systems is not valid [43]. In order to describe the behaviour of the VW when $\beta < 0.1$, we used numerical methods (figs. 4a,b).

7. Estimation of the lower bound of electrode length where VW = 0: L_D

The critical electrode length that supports a non-zero VW is potentially interesting. Specifically, if this electrode length is sensitive to medium properties, it may suggest a means for improving the stability of an excitable medium with respect to vulnerability. The transition point where the VW switches from a zero value to a nonzero value is determined by the critical electrode length, L_D, necessary for initiating a unidirectionally propagated wavefront. The critical length L_D is a function of the recovery variable in the vicinity of the electrode, i.e. $L_D = L_D(V)$. The greater the value of $V(x_m, t_{test})$ that the midpoint of the electrode at $x = x_m$ "sees", the smaller the length of L_D.

We must find the appropriate time delay T for

test stimulus to diminish L_D while maintaining unidirectional conduction. For example, while we may be able to successfully excite the medium with length $L_D(V_m)$, it may be possible to find a smaller critical length that permits successful unidirectional excitation by simply changing the time of the test stimulation $V(x_m, t_{test} + T) > V_m$. What is the maximum value of T? This is determined by the VW boundary separating unidirectional and bidirectional propagation.

Let us consider test stimulation at $t = t_{test}$ which initiates unidirectional conduction. Let $t_{test} = t_m + T$, where as mentioned above, t_m, is the time when S passes the midpoint of the electrode (fig. 6). Let $T = T_2$ (fig. 6b) which is the transition point between unidirectional and bidirectional propagation. This is the maximum time delay associated with the minimum critical length, $L_D(V_{T_2})$, where $V_{T_2} = V(x_m, t_m + T_2)$. Unidirectional propagation will fail if the time delay is less than T_2 since $V(x_m, t_{sim} + T_2 - \delta) < V_{T_2}$, $\delta > 0$, and only bidirectional conduction will be observed for $\delta < 0$.

We estimate this value of L_D by balancing the "charge" available in the electrode region with the flow of charge into the fronts and the amount of charge that must be "replaced" due to the incomplete recovery process. This approach has been developed in ref. [44], where the authors estimated the conditions for ignition of a flame associated with a departure from near equilibrium conditions. In order to initiate unidirectional conduction at the VW boundary when $T = T_2$, the amount of charge, $(m_3 - m_1)L_D\,\Delta t$, produced by a test stimulus during the time interval, Δt, must be equal to the sum of the charge flow into the wavefronts of a fully developed test impulse (as approximated by the gradient over the distance, L_{crit}), $2(m_3 - m_1)\,\Delta t/L_{crit}$, and the amount of charge that must be replaced due to incomplete recovery, $(V_{eq} - V_{crit})CT_2\,\Delta t$. Equating these values, we find that:

$$(m_3 - m_1)L_D\,\Delta t = \frac{2(m_3 - m_1)}{L_{crit}}\Delta t + (V_{eq} - V_{crit})CT_2\,\Delta t\,.$$

Transforming this balance equation, we find

$$L_D = \frac{2}{L_{crit}} + \frac{V_{eq} - V_{crit}}{m_3 - m_1}CT_2\,. \tag{30}$$

Replacing T_2 with eq. (28), yields

$$L_D = \left(\frac{2}{L_{crit}} + \frac{V_{eq} - V_{crit}}{m_3 - m_1}\frac{1-\xi}{1+\xi}L_{crit}\right) \times \left(1 + \frac{V_{eq} - V_{crit}}{m_3 - m_1}\frac{2-\xi}{2(1+\xi)}\right)^{-1}. \tag{31}$$

For our computations, $V_{eq} - V_{crit} = 1.5$ and $m_3 - m_1 = 3.6$ and $L_{crit} = 6.25$. From eq. (31), the estimate of $L_D = 1.38$ so that the ratio: $L_D/L_{crit} = 0.22$, which coincides with the numerically determined value shown in fig. 7.

In this particular numeric example L_D relates to more than one and less than five actual cell lengths for the atrium, and more than two and less than seven actual cell lengths for the ventricle.

Note that eq. (31), can be written in a slightly more general form by replacing V_{crit} with $V(x_m, t_{test})$ and L_{crit} by the wavefront thickness associated with $V(x_m, t_{test})$. For instance, if $V(x_m, t_{test}) = V_{eq}$, then $L_D = 2/L_0$, the minimum length that must be excited in order to achieve any propagation. In this case L_D relates to one actual cell length for both atrium and ventricle.

8. Discussion

Why is vulnerability in an excitable medium interesting? A variety of different classes of spiral wavefronts have been observed in excitable media – most notably, the BZ medium [45–48]. These wavefronts have been the source of great fascination because a supposedly homogeneous medium can reveal highly organized patterns, e.g. a continuously recycling spiral wavefront – that exhibits a degree of organization that at first glance seems hard to accept. This apparently organized activity lacks any source of central coordination and reflects the simplest coupling of elemental reaction processes

by spatial diffusion. While spiral patterns appear to serve no apparent function in BZ, their appearance in cardiac tissue [5,6] and as waves of calcium concentration within a cell [49] may serve some important signaling functions. While it has been long recognized that spiral waves can be initiated by disturbing the medium, the conditions of the disturbance have never been critically explored. Because of the emerging importance of spiral wave initiation, particularly in cardiac tissue, we feel it is important to explore the initiating events that can eventually lead to spiral wave formation.

Control of spiral initiation, maintenance and termination may be important processes to understand. Although speculative, it is interesting to consider the results of a recently terminated clinical trial, CAST [7]. Several drugs were tested as to their ability to prevent potentially life-threatening cardiac rhythms (tachycardia and ventricular fibrillation) in a large number of subjects that had recently survived a heart attack (possibly a transient or permanent block of a coronary artery, leading to damaged cardiac tissue). The underlying model and hypothesis can be briefly summarized as follows.

Following a heart attack, cardiac tissue may be damaged rendering the heart subject to rhythm disturbances. One potential hypothesis was that damaged tissue may occasionally initiate a local excitation that spreads to the rest of the heart. As has been shown by many investigators and as we have discussed above, the timing of this "extra" stimulus could produce a discontinuous wavefront such that the resultant wavefront recirculates for long periods of time. Normally, continuous wavefronts originating at a stimulation source travel away from the stimulation site and eventually collide in a remote region of the heart. With reentrant excitation (spiral waves), the heart rate becomes that of the spiral rotation period and if this is quite rapid, the pumping action of the heart can be compromised with the possibility of fainting or sudden cardiac death.

Drugs that block the cardiac sodium channel act in a manner that prolongs the refractory period – the time when cardiac cells do not respond to stimulation. Consequently these drugs are often recommended for patients in order to suppress "extra" stimulation pulses originating in injured tissue. An implied hypothesis of the CAST study was that extra stimuli in the presence of drug are no more malignant than extra stimuli in the absence of drug. Although drug dosage was adjusted to achieve >80% suppression of extra stimuli, the results of the study argue against this hypothesis.

Sodium channel blockade is equivalent to reducing the amplitude of the function, $f(u)$, which reduces the trigger wave velocity (eq. (14)). Thus while these drugs can indeed reduce the incidence of extra stimuli (by reducing excitability and hence increasing the refractory period), they, in parallel, increased the vulnerable window (figs. 8–10) by slowing the propagation velocity. Similar behavior was described in our earlier numerical and experimental studies [8,9,31]. The surprise from the CAST results was that two of the three treated groups experienced a significant increase (3x) in the rate of sudden cardiac death (supposedly from life-threatening arrhythmias) when compared with the untreated group. The CAST results, however, are consistent with the mechanism of vulnerability illustrated in our studies. The parallels between the CAST results and our theoretical results indicate the possibility of linking molecular (e.g. blockade of sodium and potassium channels in cardiac cell membrane) with macroscopic events (e.g. initiation of potentially life-threatening disturbances in cardiac rhythm).

Our results suggest that for large electrodes, the VW can be approximated by the length of time required for V_{crit} to propagate across an electrode of length L_S. However, for stimulation electrodes of the order of the wavefront thickness, the sensitivity of the VW to L_S is reduced as shown by the boundary layer corrections. Here, we found that the singular limit approximation, $VW^{(0)}$, may underestimate the correct VW by a factor or 2 or 3 when the source of stimulation is less than that of the front thick-

ness. For electrodes associated with devices such as pacemakers and defibrillators, these differences can be ignored, but for stimulation from aberrant cells, these differences may be important.

An unexpected result from our analysis was the nature of the minimum excited length necessary to display vulnerability. For the Fitzhugh–Nagumo parameters we used, this value was a fraction of the front thickness when $V = V_{crit}$ and comparable in size to a few cardiac cells. The critical length is dependent on all medium properties and thus it may be possible to design physiologic interventions that reduce vulnerability by increasing this critical mass.

In summary, we have shown that the vulnerable window is a generic property of Fitzhugh–Nagumo-like excitable media and depends on basic medium parameters. To explore the VW, we developed a method for solving linearized Fitzhugh-Nagumo-like equations during wavefront formation under nonstationary conditions. With these results, we computed a correction to the singular limit estimate of the VW that revealed interesting properties for small electrodes. These results may be useful in designing interventions for control of spiral wave initiation, particularly with respect to anticipating drug effects on cardiac rhythms.

Acknowledgements

We wish to acknowledge the critical assistance provided by James P. Keener and Valentin I. Krinsky. Their careful review was most helpful in the development, interpretation and explanation of our results.

References

[1] C.J. Wiggers and R. Wegria, Ventricular fibrillation due to a single localized induction and condenser shocks applied during the vulnerable phase of ventricular systole, Am. J. Physiol. 128 (1939) 500–505.

[2] J. Roelandt, P. Klootwijk, J. Kubsen and J.J. Janse, Sudden death during longterm ambulatory monitoring, Eur. Heart J. 5 (1984) 7–20.

[3] A.T. Winfree, When time breaks down: The three-dimensional dynamics of electrochemical waves and cardiac arrhythmias (Princeton Univ. Press, Princeton, 1987).

[4] F.B. Gul'ko and A.A. Petrov, Mechanism of the formation of closed pathways of conduction in excitable media, Biofizika 17 (1972) 261–270.

[5] F.J. van Capelle and D. Durrer, Computer simulation of arrhythmias in a network of coupled excitable elements, Circulation Res. 47 (1980) 117–124.

[6] J.M. Davidenko, P. Kent, D.R. Chialvo, D.C. Michaels and J. Jalife, Sustained vortex-like waves in normal isolated ventricular muscle, Proc. Natl. Acad. Sci. USA 87 (1990) 8785–8790.

[7] The Cardiac Arrhythmia Suppression Trial (CAST) Investigators, Preliminary report: effect of encainide and flecainide on mortality in a randomized trial of arrhythmia suppression after myocardial infarction, N. Engl. J. Med. 321 (1989) 406–412.

[8] C.F. Starmer, A.A. Lastra, V.V. Nesterenko and A.O. Grant, Proarrhythmic response to sodium channel blockade: Theoretical model and numerical experiments, Circulation 84 (1991) 1364–1377.

[9] V.V. Nesterenko, A.A. Lastra, L.V. Rosenshtraukh and C.F. Starmer, A proarrhythmic response to sodium channel blockade: Modulation of the vulnerable period in guinea pig ventricular mypocardium, J. Card. Pharm. 19 (1992) 810–820.

[10] I.S. Belakhovski, Several modes of excitation movement in ideal excitable tissue, Biofizika 10 (1965) 1063–1067.

[11] V.I. Krinsky, Spread of excitation in an inhomogeneous medium (rate similar to cardiac fibrillation), Biofizika 11 (1966) 676–683.

[12] N. Wiener and A. Rosenblueth, The mathematical formulation of the problem of conduction of impulses in a network of connected excitable elements, specifically in cardiac muscle, Arch. Inst. Cardiologia Mexico 16 (1946) 205–265.

[13] V.S. Zykov, Stationary and nonstationary circulations of excitation, in: Autowave Processes in Systems with Diffusion (IPF AN USSR, Gorki, 1981).

[14] R.N. Khramov, Circulation of a pulse in an excitable medium. The critical dimension of a closed contour, Biofizika 23 (1978) 879–885.

[15] A.M. Pertsov, E.A. Ermakova and A.V. Panfilov, Rotating spiral waves in a modified Fitzhugh–Nagumo model, Physica D 14 (1984) 117–124.

[16] A.S. Mikhailov and V.I. Krinky, Reverberator in an active medium. Analytic results, Biofizika 5 (1982) 919–925.

[17] J.P. Keener and J.J. Tyson, Spiral waves in the Belousov–Zhabotinskii reaction, Physica D 21 (1986) 300–324.

[18] A.V. Panfilov and A.V. Holden, Vortices in a system of two coupled excitable fibers, Phys. Lett. A 147 (1990) 463–466.
[19] A. Palmer, J. Brindley and A.V. Holden, Initiation and stability of reentry in two coupled excitable fibers, Bull. Math. Biol. 54 (1992) 1039–1056.
[20] M.A. Allessie, F.I.M. Bonke and F.J.G. Schopoman, Circus movement in rabbit atrial muscle as a mechanism of tachycardia – III. The "leading circle" concept: a new model of circus movement in cardiac tissue without the involvement of anatomical obstacle, Circulation Res. 41 (1973) 9–18.
[21] N.I. Kukushkin and M. Ye. Sakson, Prediction of the vulnerability of the ventricle to arrhythmia with latency and the duration of the extrasystolic response, Biofizika 16 (1971) 941–947.
[22] H.J.J. Wellens, R.M. Schuilenbur and D. Durrer, Electrical stimulation of the heart in patients with ventricular tachycardia, Circulation 46 (1972) 216.
[23] H.A. Fozzard, E. Haber, R.B. Jennings, A.M. Katz and H.E. Morgan, The Heart and Cardivascular System, Scientific Foundations, Vol. 1 (Raven Press, New York, 1991).
[24] Y. Sakamoto and M. Goto, A study of the membrane constants in the dog miocardium, Jpn. J. Physiol. 20 (1970) 30–41.
[25] S. Weidmann, Electrical constants of trabecular muscle from mammalian heart, J. Physiol. 210 (1970) 1041–1054.
[26] D.C. Chang, I. Tasaki, W.J. Adelman and H.R. Leuchtag, Structure and function in excitable cells (Plenum, New York, 1983).
[27] V.I. Krinskii and Yu.M. Kokoz, Analysis of equations of excitable membranes. I. Reduction of the Hodgkin–Huxley equations to a second-order system, Biofizika 18 (1973) 533–539.
[28] F.R. Gilliam, C.F. Starmer, and A.O. Grant, Blockade of rabbit atrial sodium channels by lidocaine: characterization of continuous and frequency-dependent blocking, Circulation Res. 65 (1989) 723–739.
[29] T.J. Colatsky, C.H. Follmer and C.F. Starmer, Channel specificity in antiarrhythmic drug action: mechanism of potassium channel block and its role in suppressing and aggravating cardiac arrhythmias, Circulation 82 (1990) 2235–2242.
[30] F.R. Gilliam, P.A. Rivas, D.J. Wendt, C.F. Starmer and A.O. Grant, Extracellular pH modulates the block of both sodium and calcium channels by nicardipione, Am. J. Physiol. 259 (1990) H1178–H1184.
[31] C.F. Starmer, A.R. Lancaster, A.A. Lastra and A.O. Grant, Cardiac instability amplified by use-dependent Na channel blockade, Am. J. Physiol. 262 (1992) H1305–H1310.
[32] C.F. Starmer, D.N. Romashko, V.N. Biktashev, M.R. Stepanov, O.N. Makarova and V.I. Krinsky, Vulnerability in a homogeneous excitable medium: analytical and numerical studies, Biophys. J., accepted.
[33] J.J. Tyson and J.P. Keener, Singular perturbation theory of traveling waves in excitable media (a review), Physica D 32 (1988) 327–361.
[34] A.S. Mikhailov, Foundations of Synergetics 1. Distributed Active Systems (Springer, Berlin, 1990).
[35] L.A. Ostrovskii and V.G. Yakhno, Formation of pulses in an excitable medium, Biofizika 20(3) (1975) 498–503.
[36] J.P. Keener, Waves in excitable media, SIAM J. Appl. Math. 39 (1980) 528–548.
[37] V.S. Markin, V.F. Pastushenko and Yu.A. Chizmadzhev, Theory of excitable media (Nauka, Moscow, 1981) (in Russian).
[38] J. Rinzel and J.B. Keller, Traveling wave solutions of a nerve conduction equation, Biophys. J. 13 (1973) 1313–1337.
[39] V.S. Zykov, Simulation of Wave Processes in Excitable Media (Manchester Univ. Press, Manchester, 1987).
[40] J. Nagumo, S. Yoshizawa and S. Arimoto, Bistable transmission lines, IEEE Trans. Circuit Theory 12 (1965) 400–412.
[41] V.G. Yakhno, Calculation of wave velocity in an excitable medium, Biofizika 21 (1976) 562–566.
[42] G.K. Batchelor, An Introduction to Fluid Dynamics (Cambridge Univ. Press, Cambridge, 1970).
[43] V.G. Yakhno, A model of the leading centre, Biofizika 20 (1975) 679–684.
[44] Ya.B. Zeldovich, G.I. Barenblatt, V.B. Librovich and G.M. Makhviladze, The mathematical theory of combustion and explosions (Consultants Bureau, New York, 1985).
[45] A.M. Zhabotinsky and A.N. Zaikin, in: Oscillatory Processes in Biological and Chemical Systems (Science Publ. Pushchino, Russia, 1971) (in Russian) p. 279.
[46] A.T. Winfree, Spiral waves of chemical activity, Science 175 (1972) 634–636.
[47] K.I. Agladze and V.I. Krinsky, Multiarmed vortices in an active chemical medium, Nature 296 (1982) 424–426.
[48] A.M. Pertsov, R.R. Aliev and V.I. Krinsky, Three-dimensional twisted wortices in an excitable chemical medium, Nature 345 (1990) 419–421.
[49] J. Lechleiter, S. Girard, E. Peralta and D. Clapham, Spiral calcium wave propagation and annihilation in Xenopus laevis oocytes, Science 252 (1991) 123–126.